COBEM 2023 27TH INTERNATIONAL CONGRESS OF MECHANICAL ENGENEERING

ABCM Brazilian Society of Mechanical Sciences and Engineering
27th ABCM International Congress of Mechanical Engineering
December 04-08, 2023, Florianópolis-SC, Brazil

COBEM2023-2181
NUMERICAL ANALYSIS OF DISSIPATION IN A LARGE STRAIN THERMO-VISCOELASTIC CONSTITUTIVE MODEL

Péricles R. P. Carvalho
Rodolfo A. K. Sanches
Department of Structural Engineering, São Carlos School of Engineering, University of São Paulo.
Av. Trab. São Carlense, 13566-590, São Carlos, São Paulo, Brazil
periclescarvalho@usp.br, rodolfo.sanches@usp.br

Abstract. *We present a phenomenological large strain thermo-viscoelastic constitutive model, using a total Lagrangian kinematic description based on the multiplicative decomposition of the thermal, elastic and viscous deformation gradients. The model is defined by a Helmholtz free energy, and is thermodynamically-based, meaning that the constitutive equations are derived from the laws of thermodynamics. The thermal component is calculated by an isotropic expansion law in exponential form. The viscoelastic part is represented by Zener's rheological model. For the elastic part, we apply a neo-Hookean constitutive model. To account for the viscous behaviour, an internal variable model is applied, that is, the viscous deformations are stored as internal variables and updated using the evolution laws, written in terms of the rate of viscous deformation gradient. The equation of heat conduction is derived from the first law of thermodynamics, including the heat generated by viscous dissipation, and the relation between heat fluxes and temperatures is given by Fourier's law. The constitutive model is applied to a strain-stress example of uniaxial monotonic loading over different strain and stress rates. Graphs such as mechanical dissipation and energy rates over time are presented for each case to characterize the dissipative behaviour of the problem.*

Keywords: *Dissipation, viscoelasticity, thermo-viscoelasticity, large strain, thermo-mechanical*

1. INTRODUCTION

The damping and impact absorption properties of viscoelastic materials make them valuable for many practical applications in engineering, especially in the large strain context. One common way to simulate numerically these materials is by the internal variable method (IVM), where the viscous behavior is represented by evolution laws written in terms of the viscous deformation rates. For large strain problems, this strategy is often applied together with a multiplicative decomposition between elastic and viscous deformation gradients (Huber and Tsakmakis, 2000; Bonet, 2001; Pascon and Coda, 2017; Carvalho *et al.*, 2023).

In this work, we propose an extension of these models for the thermo-viscoelastic case, considering an additional multiplicative decomposition between thermal and mechanical deformation gradients. We base our model in a consistent thermodynamic framework, following the general idea of Vujošević and Lubarda (2002), which focused on thermo-elastic models. In this case, however, we must take into account the energy dissipation and heat generated by the inelastic mechanisms of the material. According to Kamlah and Haupt (1997), only a fraction of the dissipated mechanical energy is stored in structural changes of the material, whereas the rest is converted into heat. According to Rosakis *et al.* (2000), it is customary to assume the heating fraction to be a constant between 80% and 100%. However, the experiments from Mason *et al.* (1994) prove that, in practical terms, the fraction does vary with respect to strain and strain rates. Since the present work is focused only on the theoretical scope of the proposed model, we consider that fraction to be always 100%, i.e. all dissipated energy is converted into heat.

2. KINEMATICS

Let Ω_0 and Ω_1 denote the initial (undeformed) and current (deformed) configurations of a domain, respectively, and let $\mathbf{F}$ denote the deformation gradient from Ω_0 to Ω_1. We define the jacobian (or volumetric strain), the right Cauchy-Green stretch and the velocity gradient, respectively, as

$$J = \det \mathbf{F}, \tag{1}$$

$$\mathbf{C} = \mathbf{F}^T\mathbf{F}, \text{ and} \tag{2}$$

$$\mathbf{L} = \dot{\mathbf{F}}\mathbf{F}^{-1}. \tag{3}$$

For thermo-mechanical problems, let us assume that there is a intermediate configuration Ω_t where only thermal strains are present, and let $\mathbf{F}_t$ denote the thermal deformation gradient, mapping from Ω_0 to Ω_t. Consequently, mapping

from Ω_t to Ω_1 we have the mechanical deformation gradient, denoted here by $\mathbf{F}_m$, and the total deformation gradient can be written by the multiplicative decomposition $\mathbf{F} = \mathbf{F}_m\mathbf{F}_t$.

Analogously, considering a viscoelastic model for the mechanical part of the deformation gradient, and assuming a viscous intermediate configuration Ω_v, we can write $\mathbf{F}_m = \mathbf{F}_e\mathbf{F}_v$, where $\mathbf{F}_e$ and $\mathbf{F}_v$ are the elastic and viscous deformation gradients, respectively.

Considering an isotropic thermal expansion model, we can write the thermal deformation gradient as $\mathbf{F}_t = \lambda_t\mathbf{I}$, where $\mathbf{I}$ is the identity tensor, and λ_t is a scalar value named thermal stretch. Therefore, the total deformation gradient can be written as

$$\mathbf{F} = \lambda_t\mathbf{F}_m = \lambda_t\mathbf{F}_e\mathbf{F}_v. \tag{4}$$

For each component of the deformation gradient (elastic, viscous, thermal and mechanical), we can define respective jacobians, right Cauchy-Green stretch tensors, and velocity gradients, using expression completely analogous to Eqs. (1), (2) and (3), but denoted with their respective indexes. Particularly, we can define:

$$\mathbf{C}_e = \mathbf{F}_e^T\mathbf{F}_e = (\lambda_t^{-1}\mathbf{F}_v^{-T}\mathbf{F}^T)(\lambda_t^{-1}\mathbf{F}\mathbf{F}_v^{-1}) = \lambda_t^{-2}\mathbf{F}_v^{-T}\mathbf{C}\mathbf{F}_v^{-1}, \tag{5}$$

$$\mathbf{C}_m = \mathbf{F}_m^T\mathbf{F}_m = \mathbf{F}_v^T\mathbf{F}_e^T\mathbf{F}_e\mathbf{F}_v = \mathbf{F}_v^T\mathbf{C}_e\mathbf{F}_v = \lambda_t^{-2}\mathbf{C}, \quad \text{and} \tag{6}$$

$$\mathbf{L}_v = \dot{\mathbf{F}}_v\mathbf{F}_v^{-1}. \tag{7}$$

Then, with some algebraic manipulation, we can express the rate of the mechanical and elastic right Cauchy-Green stretch tensors as

$$\dot{\mathbf{C}}_m = \lambda_t^{-2}\dot{\mathbf{C}} - 2\,\lambda_t^{-1}\dot{\lambda}_t\mathbf{C}_m, \quad \text{and} \tag{8}$$

$$\dot{\mathbf{C}}_e = \lambda_t^{-2}\mathbf{F}_v^{-T}\dot{\mathbf{C}}\mathbf{F}_v^{-1} - 2\,\lambda_t^{-1}\dot{\lambda}_t\mathbf{C}_e - 2\,\mathrm{sym}(\mathbf{C}_e\mathbf{L}_v), \tag{9}$$

where sym $(\cdot)$ denotes the symmetric part of a tensor.

3. THERMO-VISCOELASTIC MODEL

The present model is thermodynamically-based, meaning that it derives from the laws of thermodynamics. Using a total Lagrangian description, the first and second laws of thermodynamics can be written in local form as

$$\dot{\psi} + T\dot{\eta} + \dot{T}\eta - R = \frac{1}{2}\,\mathbf{S} : \dot{\mathbf{C}} - \boldsymbol{\nabla}_0 \cdot \mathbf{q}_0, \tag{10}$$

$$d_{int} = \frac{1}{2}\,\mathbf{S} : \dot{\mathbf{C}} - \dot{\psi} - \dot{T}\eta - \frac{1}{T}\mathbf{q}_0 \cdot \boldsymbol{\nabla}_0 T \geq 0. \tag{11}$$

where ψ is the helmholtz energy, T is the temperature, η is the entropy, R the internal heat by time, $\mathbf{S}$ is the second Piola-Kirchhoff stress, $\boldsymbol{\nabla}_0$ is the gradient in the initial configuration, $\mathbf{q}_0$ is the heat flux in the initial configuration, and d_{int} is the dissipation rate. We note that, in this work, the variables ψ, η, R and d_{int} are defined per unit volume at the initial configuration, as opposed to common formulations where they are defined per unit mass, and must be multiplied by the initial density to maintain the consistency of the expressions.

It can be proven that $\boldsymbol{\nabla}_0 T = \mathbf{F}^T\boldsymbol{\nabla} T$, where $\boldsymbol{\nabla}$ denotes the gradient with respect to the current configuration. Furthermore, $\mathbf{q}_0$ can be related to the heat flux in the current configuration ($\mathbf{q}$) by the expression $\mathbf{q}_0 = J\mathbf{F}^{-1}\mathbf{q} = J\mathbf{q}\mathbf{F}^{-T}$. So, the following relation between the Lagrangian and Eulerian forms can be obtained:

$$\mathbf{q}_0 \cdot \boldsymbol{\nabla}_0 T = J(\mathbf{q}\mathbf{F}^{-T}) \cdot (\mathbf{F}^T\boldsymbol{\nabla} T) = J\mathbf{q} \cdot \boldsymbol{\nabla} T. \tag{12}$$

The helmholtz free energy of the present model is composed by a mechanical part (ψ_m), written in terms of the mechanical strain, and a thermal part (ψ_t), written in terms of the temperature. Due to the adopted kinematics, however, the mechanical strains are defined in the thermal intermediate configuration (Ω_t), and, consequently, so is the mechanical helmholtz energy. To apply it into a total Lagrangian formulation, we must change it to the initial configuration Ω_0. Therefore, we multiply the mechanical helmholtz energy by $J_t = \det\mathbf{F}_t = \det(\lambda_t\mathbf{I}) = \lambda_t^3$ (Vujošević and Lubarda, 2002). The total helmholtz energy can then be written as

$$\psi = \lambda_t^3\psi_m(\mathbf{C}_m) + \psi_t(T). \tag{13}$$

The mechanical part in this work is represented by a viscoelastic model, using Zener's rheological model as basis (Pascon and Coda, 2017). This model consists of two components for the Helmholtz energy: one depending only on the elastic strain (denoted by ψ_e), and the other depending of the total mechanical strain (denoted by ψ_e^∞). That is,

$$\psi_m = \psi_e(\mathbf{C}_e) + \psi_e^\infty(\mathbf{C}_m). \tag{14}$$

Assuming that λ_t depends only on the temperature, the rate of the total Helmholtz energy can be calculated as

$$\dot{\psi} = \lambda_t^3 \left(\frac{\partial \psi_e^\infty}{\partial \mathbf{C}_m} : \dot{\mathbf{C}}_m + \frac{\partial \psi_e}{\partial \mathbf{C}_e} : \dot{\mathbf{C}}_e \right) + \left(\frac{\partial \psi_t}{\partial T} + 3\lambda_t^2 \psi_m \frac{\partial \lambda_t}{\partial T} \right) \dot{T}. \tag{15}$$

From Eqs. (8) and (9), we have

$$\frac{\partial \psi_e^\infty}{\partial \mathbf{C}_m} : \dot{\mathbf{C}}_m = \lambda_t^{-2} \frac{\partial \psi_e^\infty}{\partial \mathbf{C}_m} : \dot{\mathbf{C}} - 2\,\lambda_t^{-1} \dot{\lambda}_t \frac{\partial \psi_e^\infty}{\partial \mathbf{C}_m} : \mathbf{C}_m = \lambda_t^{-2} \frac{\partial \psi_e^\infty}{\partial \mathbf{C}_m} : \dot{\mathbf{C}} - \lambda_t^{-1}\, \text{tr}\,(\mathbf{M}_m) \frac{\partial \lambda_t}{\partial T} \dot{T} \quad \text{and} \tag{16}$$

$$\begin{aligned} \frac{\partial \psi_e}{\partial \mathbf{C}_e} : \dot{\mathbf{C}}_e &= \frac{\partial \psi_e}{\partial \mathbf{C}_e} : \left(\lambda_t^{-2} \mathbf{F}_v^{-T} \dot{\mathbf{C}} \mathbf{F}_v^{-1} \right) - \frac{\partial \psi_e}{\partial \mathbf{C}_e} : \left(2\,\lambda_t^{-1} \dot{\lambda}_t \mathbf{C}_e \right) - 2\, \frac{\partial \psi_e}{\partial \mathbf{C}_e} : \text{sym}(\mathbf{C}_e \mathbf{L}_v) \\ &= \left(\lambda_t^{-2} \mathbf{F}_v^{-1} \frac{\partial \psi_e}{\partial \mathbf{C}_e} \mathbf{F}_v^{-T} \right) : \dot{\mathbf{C}} - \lambda_t^{-1}\, \text{tr}\,(\mathbf{M}_e) \frac{\partial \lambda_t}{\partial T} \dot{T} - \mathbf{M}_e : \mathbf{L}_v, \end{aligned} \tag{17}$$

where $\mathbf{M}_e$ and $\mathbf{M}_m$ are the so-called Mandel stresses, defined as

$$\mathbf{M}_e = 2\, \mathbf{C}_e \frac{\partial \psi_e}{\partial \mathbf{C}_e}, \tag{18}$$

$$\mathbf{M}_m = 2\, \mathbf{C}_m \frac{\partial \psi_e^\infty}{\partial \mathbf{C}_m}, \tag{19}$$

and $\text{tr}\,(\cdot)$ denotes the trace of a tensor. We note that the tensorial property $\text{tr}\,(\mathbf{AB}) = \mathbf{A}^T : \mathbf{B} = \mathbf{A} : \mathbf{B}^T$ was used.

Applying Eqs. (16) and (17) into (15), and then into Eq. (10), the first law of thermodynamics can be rewritten as

$$\begin{aligned} &\left(\frac{1}{2}\, \mathbf{S} - \lambda_t \frac{\partial \psi_e^\infty}{\partial \mathbf{C}_m} - \lambda_t \mathbf{F}_v^{-1} \frac{\partial \psi_e}{\partial \mathbf{C}_e} \mathbf{F}_v^{-T} \right) : \dot{\mathbf{C}} - \left[\eta + \frac{\partial \psi_t}{\partial T} + 3\lambda_t^2 \psi_m \frac{\partial \lambda_t}{\partial T} - \lambda_t^2 \left(\text{tr}\, \mathbf{M}_m + \text{tr}\, \mathbf{M}_e \right) \frac{\partial \lambda_t}{\partial T} \right] \dot{T} \\ &+ \lambda_t^3\, \mathbf{M}_e : \mathbf{L}_v - T\dot{\eta} - R - \boldsymbol{\nabla}_0 \cdot \mathbf{q}_0 = 0, \end{aligned} \tag{20}$$

and applying into Ineq. (11), the second law of thermodynamics can be rewritten as

$$\begin{aligned} d_{int} = &\left(\frac{1}{2}\, \mathbf{S} - \lambda_t \frac{\partial \psi_e^\infty}{\partial \mathbf{C}_m} - \lambda_t \mathbf{F}_v^{-1} \frac{\partial \psi_e}{\partial \mathbf{C}_e} \mathbf{F}_v^{-T} \right) : \dot{\mathbf{C}} - \left[\eta + \frac{\partial \psi_t}{\partial T} + 3\lambda_t^2 \psi_m \frac{\partial \lambda_t}{\partial T} - \lambda_t^2 \left(\text{tr}\, \mathbf{M}_m + \text{tr}\, \mathbf{M}_e \right) \frac{\partial \lambda_t}{\partial T} \right] \dot{T} \\ &+ \lambda_t^3\, \mathbf{M}_e : \mathbf{L}_v - \frac{1}{T} \mathbf{q}_0 \cdot \boldsymbol{\nabla}_0 T \geq 0. \end{aligned} \tag{21}$$

Since $\dot{\mathbf{C}}$ and $\dot{T}$ are arbitrary for thermodynamic processes, the following constitutive relations must be fulfilled for the second Piola-Kirchhoff stress and the entropy:

$$\mathbf{S} = 2\lambda_t \frac{\partial \psi_e^\infty}{\partial \mathbf{C}_m} + 2\lambda_t \mathbf{F}_v^{-1} \frac{\partial \psi_e}{\partial \mathbf{C}_e} \mathbf{F}_v^{-T}, \quad \text{and} \tag{22}$$

$$\eta = -\frac{\partial \psi_t}{\partial T} + \lambda_t^2 \left(\text{tr}\, \mathbf{M}_m + \text{tr}\, \mathbf{M}_e - 3\psi_m \right) \frac{\partial \lambda_t}{\partial T}. \tag{23}$$

Furthermore, we adopt the following evolution law for the viscous part:

$$\mathbf{L}_v = \frac{1}{\eta} \mathbf{M}_e^D \quad \Rightarrow \quad \dot{\mathbf{F}}_v = \frac{1}{\eta} \mathbf{M}_e^D \mathbf{F}_v, \tag{24}$$

where η is the viscosity parameter, and $(\cdot)^D$ denotes the deviatoric part of a tensor. We note that this law is suitable with the second law of thermodynamics, once $\mathbf{M}_e : \mathbf{L}_v = \frac{1}{\eta} \mathbf{M}_e : \mathbf{M}_e^D = \frac{1}{\eta} \|\mathbf{M}_e^D\|^2 \geq 0$. Furthermore, it preserves the inelastic incompressibility property, that is,

$$\dot{J}_v = \frac{\partial J_v}{\partial \mathbf{F}_v} : \dot{\mathbf{F}}_v = \frac{J_v}{\eta} \mathbf{F}_v^{-T} : \left(\mathbf{M}_e^D \mathbf{F}_v \right) = \frac{J_v}{\eta} \left(\mathbf{F}_v^{-T} \mathbf{F}_v^T \right) : \mathbf{M}_e^D = \frac{J_v}{\eta}\, \mathbf{I} : \mathbf{M}_e^D = 0. \tag{25}$$

It must be noted that this incompressibility condition may be violated during the numerical solution when using certain time integrators for Eq. (24), such as the Backwards Euler method (Carvalho *et al.*, 2023). In order to overcome this issue, we apply in this work the exponential map method (Simo and Hughes, 2000; de Souza Neto *et al.*, 2011), which guarantees the incompressibility condition independently of the adopted time discretization.

By applying Eqs. (22), (23) and (24) into Eq. (20) and Ineq. (21), the first and second laws of thermodynamics can be written, respectively, in the forms

$$d_m - T\dot{\eta} + R - \boldsymbol{\nabla}_0 \cdot \mathbf{q}_0 = 0, \quad \text{and} \tag{26}$$

$$d_{int} = d_m - \frac{1}{T}\mathbf{q}_0 \cdot \boldsymbol{\nabla}_0 T \geq 0, \tag{27}$$

where d_m is the mechanical dissipation rate per volume at the initial configuration, calculated in this case by the expression

$$d_m = \frac{\lambda_t^3}{\eta}\|\mathbf{M}_e^D\|^2. \tag{28}$$

Interestingly, when comparing Eqs. (26) and (10), one can obtain the following relation

$$\frac{1}{2}\,\mathbf{S} : \dot{\mathbf{C}} = \dot{\psi} + d_m + \dot{T}\eta, \tag{29}$$

that is, the internal work rate can be written as the sum of the helmholtz rate (stored energy), the mechanical dissipation rate, and an entropy term.

3.1 Specification of the constitutive laws

In order to complete the definition of the constitutive model and implement it into a numerical framework, we must specify expressions for the Helmholtz free energy and the thermal stretch. For the mechanical part of the Helmholtz free energy, we apply a neo-Hookean model, which reads

$$\psi_e = \frac{G_e}{2}\left(\operatorname{tr}\mathbf{C}_e - 3 - 2\,\ln J_e\right), \quad \text{and} \tag{30}$$

$$\psi_e^\infty = \frac{\Lambda}{2}(\ln J_m)^2 + \frac{G_e^\infty}{2}\left(\operatorname{tr}\mathbf{C}_m - 3 - 2\,\ln J_m\right), \tag{31}$$

where Λ, G_e^∞ and G_e are the Lamé parameters of the material, and $J_e = \det\mathbf{F}_e$ and $J_m = \det\mathbf{F}_m$ are the elastic and mechanical Jacobians. We note that, due to the inelastic incompressibility condition, $J_m = J_e J_v = J_e$. Thus, the volumetric part of the model, associated with Λ, is included only in ψ_e^∞. Equations (30) and (31) result, respectively, in

$$\frac{\partial\psi_e}{\partial\mathbf{C}_e} = \frac{G_e}{2}\left(\mathbf{I} - \mathbf{C}_e^{-1}\right), \quad \text{and} \tag{32}$$

$$\frac{\partial\psi_e^\infty}{\partial\mathbf{C}_m} = \frac{\Lambda}{2}(\ln J_m)\mathbf{C}_m^{-1} + \frac{G_e^\infty}{2}\left(\mathbf{I} - \mathbf{C}_m^{-1}\right). \tag{33}$$

For the thermal part of the Helmholtz free energy, we apply the law

$$\psi_t = c\left(T - T_0 - T\ln\frac{T}{T_0}\right). \tag{34}$$

where c is the specific heat of the material, and T_0 is a reference temperature. Then, is follows that

$$\frac{\partial\psi_t}{\partial T} = -c\ln\frac{T}{T_0}. \tag{35}$$

Finally, for the thermal expansion model, we apply an exponential law which reads

$$\lambda_t = e^{\alpha(T-T_0)}, \tag{36}$$

where α is the thermal expansion coefficient of the material. This law is consistent with large strain problems, since the theoretical conditions $\lim_{T\to+\infty}\lambda_t = +\infty$ and $\lim_{T\to-\infty}\lambda_t = 0$ are fulfilled, as opposed to linear expansion models. From Eq. (36), it follows that

$$\frac{\partial\lambda_t}{\partial T} = \alpha\, e^{\alpha(T-T_0)} = \alpha\lambda_t, \tag{37}$$

4. HEAT TRANSFER

Applying Eqs. (35) and (37) into Eq. (23), the entropy can be written as

$$\eta = c \ln \frac{T}{T_0} + \alpha \lambda_t^3 \left(\operatorname{tr} \mathbf{M}_m + \operatorname{tr} \mathbf{M}_e - 3\psi_m \right). \tag{38}$$

Equation (38) can be written entirely in terms of T, $\mathbf{C}$ and $\mathbf{F}_v$. Therefore, the rate of entropy can be expressed as

$$\dot{\eta} = \frac{\partial \eta}{\partial T}\dot{T} + \frac{\partial \eta}{\partial \mathbf{C}} : \dot{\mathbf{C}} + \frac{\partial \eta}{\partial \mathbf{F}_v} : \dot{\mathbf{F}}_v = \frac{c^*}{T}\dot{T} + \mathbf{T} : \dot{\mathbf{C}} + \mathbf{T}_v : \dot{\mathbf{F}}_v \tag{39}$$

where $c^* = T\, \partial\eta/\partial T$ is the effective specific heat function, and $\mathbf{T} = \partial\eta/\partial\mathbf{C}$ and $\mathbf{T}_v = \partial\eta/\partial\mathbf{F}_v$ are thermo-mechanical coupling tensors. In the current context, these tensors are defined by relatively extensive expressions, but normally have smaller numerical order or magnitude when compared to the other terms. Thus, for simplicity, we choose to disregard the thermo-mechanical coupling tensors in our analyses. The effective specific heat is also expressed by an extensive expression, but, disregarding the terms with smaller order of magnitude, we can assume that $c^* = c$. Therefore, the rate of entropy can be written approximately as

$$\dot{\eta} \approx \frac{c}{T}\dot{T}. \tag{40}$$

Applying Eq. (40) into Eq. (26), the first law of thermodynamics can be written as:

$$d_m - c\,\dot{T} + R - \boldsymbol{\nabla}_0 \cdot \mathbf{q}_0 = 0. \tag{41}$$

This is also known as the equation of heat conduction, written here in local Lagrangian form. It can be numerically integrated using a simple backward Euler algorithm, that is, $\dot{T} = (T_{s+1} - T_s)/\Delta t$, where $(\cdot)_{s+1}$ and $(\cdot)_s$ denotes a variable taken from the current and previous step, respectively, and Δt denotes the time variation between steps. Consequently, we can express the thermal problem as follows:

$$T_{s+1} = T_s + \frac{\Delta t}{c}(d_m + R - \boldsymbol{\nabla}_0 \cdot \mathbf{q}_0)_{s+1}. \tag{42}$$

5. NUMERICAL EXAMPLES

In this work, we are only concerned with single point analyses, i.e. for each time step we solve one pair of strain and stress tensors (mechanical problem) and one temperature value (thermal problem). We assume these variables are constant throughout the analyzed domain of the proposed problem. Consequently, $\boldsymbol{\nabla}_0 \cdot \mathbf{q}_0 = 0$, and Eq. (42) can be written simply as

$$T_{s+1} = T_s + \frac{\Delta t}{c}(d_m + R)_{s+1}. \tag{43}$$

Regarding the mechanical problem, only prescribed stress is considered in the proposed example. To determine the strain at each time step, we employ a Newton-Raphson algorithm to solve numerically the non-linear constitutive relation. Our stopping criterion for convergence is set at $\|\Delta\mathbf{C}\| \leq 10^{-6}$. It's worth noting that both stress and strain are treated as fully three-dimensional symmetric tensors.

The thermo-mechanical coupling is done by a iterative partitioned method, that is: the heat conduction equation is solved separately, then the obtained temperatures are applied into the mechanical problem, which is also solved separately. Then, the temperatures are re-calculated, and this process is repeated until an adequate convergence is achieved. The adopted convergence criterion is $\|\Delta T\| \leq 10^{-4}$, where $\|\Delta T\|$ is the norm of temperature variation from the previous iteration's solution to the current one.

5.1 SIMPLE UNIAXIAL CREEP TEST

In order to show the behavior of the proposed constitutive model, we apply it to a simple uniaxial problem with controlled stress. Let us assume an simple specimen monotonically loaded with engineering stress from 0 to 20 MPa over a period t_1. Then, from t_1 to 5 s, the engineering stress is kept constant at 20 MPa. This problem is analyzed with many different values of t_1, in order to observe the influence of the stress rate on the constitutive model. For time discretization, we apply 200 steps from 0 to t_1, and 200 from t_1 to 5. Furthermore, we consider two different values of thermal expansion coefficients, $\alpha = 0.1°\mathrm{C}^{-1}$ and $\alpha = 0.03°\mathrm{C}^{-1}$, with the remaining material parameters specified in Tab. 1.

No heat is imposed to the problem besides the one generated by inelastic dissipation. Furthermore, we assume the specimen is thermally sealed, meaning that the generated heat does not dissolve into the environment. With these considerations in mind, both the mechanical and thermal problems can be solved punctually by their local equations, without the need for a more general numerical framework with domain integration.

Table 1. Parameters of the material for the simple uniaxial creep test problem

Λ (MPa)	G_e^∞ (MPa)	G_e (MPa)	η (MPa·s)	c (J/(kg °C))	k (W/(m°C))	T_0 (°C)	α (°C^{-1})
1500	10	15	8	1	10^3	25.0	variable

In Fig. 1, we show the evolution over time for the total, viscous, and thermal components of deformation gradient, in the same axis as the engineering stress is applied (assumed to be the "11" axis). For each of the two values of α, we show graphs with the results for 4 different values of t_1. From these, we can observe the influence of stress rate and thermal expansion coefficient on the problem. Naturally, the thermal stretches are higher for the case with greater α, and, to compensate that, the viscous components are smaller.

Analyzing each of the α cases independently, we note that the thermal stretch increases with the stress rate (i.e. the t_1 value), due to heat generated by the dissipation. On the other hand, viscous deformations decrease as the stress rates increase, while the total deformations tend approximately to the same value as time advances, specially for the case with $\alpha = 0.1°\text{C}^{-1}$. For the case with $\alpha = 0.03°\text{C}^{-1}$, we can observe a slight decrease on the total deformation gradient as the stress rates increase.

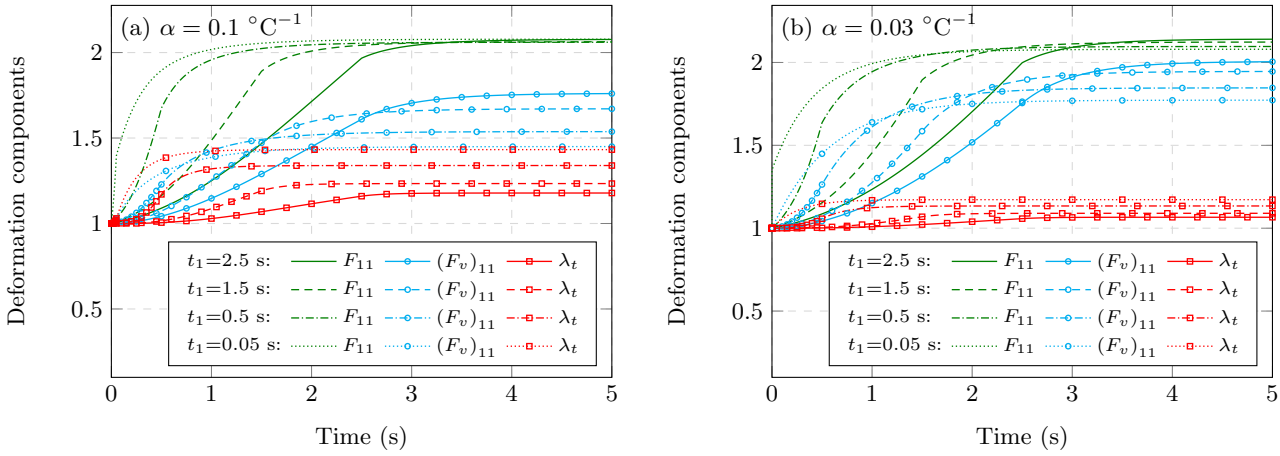

Figure 1. Deformation gradient components over time for the simple uniaxial creep test

In Figs. 2 and 3, we show the mechanical dissipation rate and mechanical dissipation over time, respectively, for each of the analyzed cases. The dissipation rate is calculated directly by Eq. (28), while the dissipation is integrated numerically by a simple algorithm that computes the areas below the curves. As already indicated by the thermal stretch values, here we can observe that, indeed, the dissipations increase with the stress rate. However, they do not increase indefinitely. Instead, they converge to a single curve with finite values. Particularly, the results for $t_1 = 5 \cdot 10^{-5}$ s and $t_1 = 5 \cdot 10^{-12}$ s are practically identical, despite the latter having a stress rate 10^7 times greater, indicating the aforementioned convergence.

Analyzing each curve individually, we note that the dissipation rates increase during the loading stage, assuming a maximum value around the time t_1, and decreasing exponentially to zero after the engineering stress is kept constant. As the dissipation rate is always positive by definition, the dissipation naturally only increases, stagnating after a certain time. Interestingly, we can also note that the dissipations and their rates are higher for the case with lower α.

To conclude this example, we show a simple analysis of work rates in Figs. 4 and 5. Using Eq. (29) as basis, we present the values over time for each of the components of the internal work rate: helmholtz rate (calculated using a simple backward Euler approach), dissipation rate, and the entropy term ($\eta\dot{T}$). Additionally, we calculate the work of external forces rate, that is, minus the applied engineering stress multiplied by $\dot{F}_{11}$. Then, the total mechanical work rate can be calculated by adding the external forces work rate and all components of the internal work rate.

These are shown for 4 different values of t_1, and both α cases. Naturally, the helmholtz rate and external forces work rate increase indefinitely as t_1 decreases. The dissipation rate, on the other hand, increases in a limited way, as already discussed previously, and the entropy term follows a similar behavior. Finally, the total mechanical work rate is constant over time and null for all cases, as theoretically expected, which serves to validate the accuracy of the calculated components, and to show the consistency of the proposed formulation.

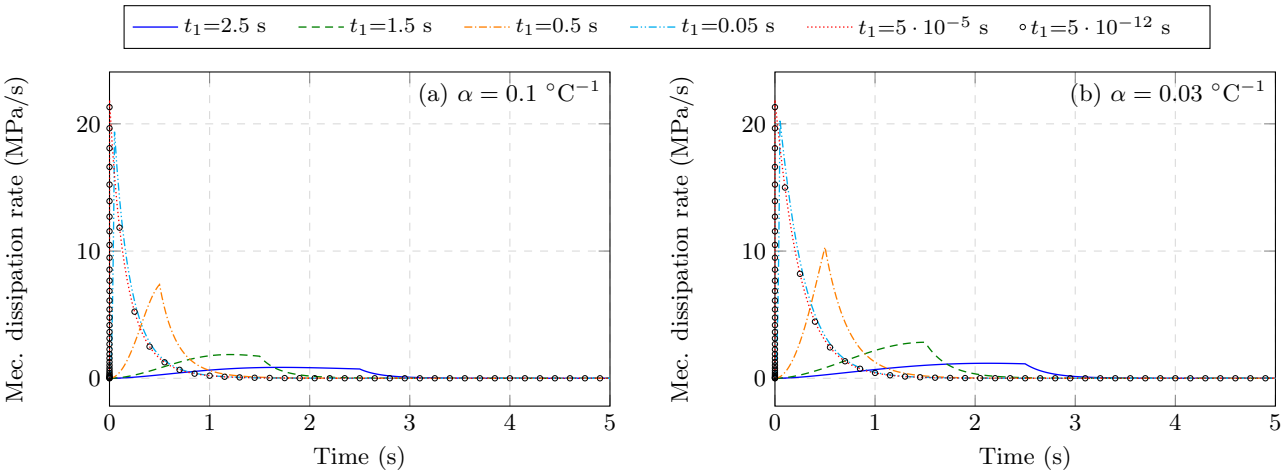

Figure 2. Mechanical dissipation rates over time for the simple uniaxial creep test

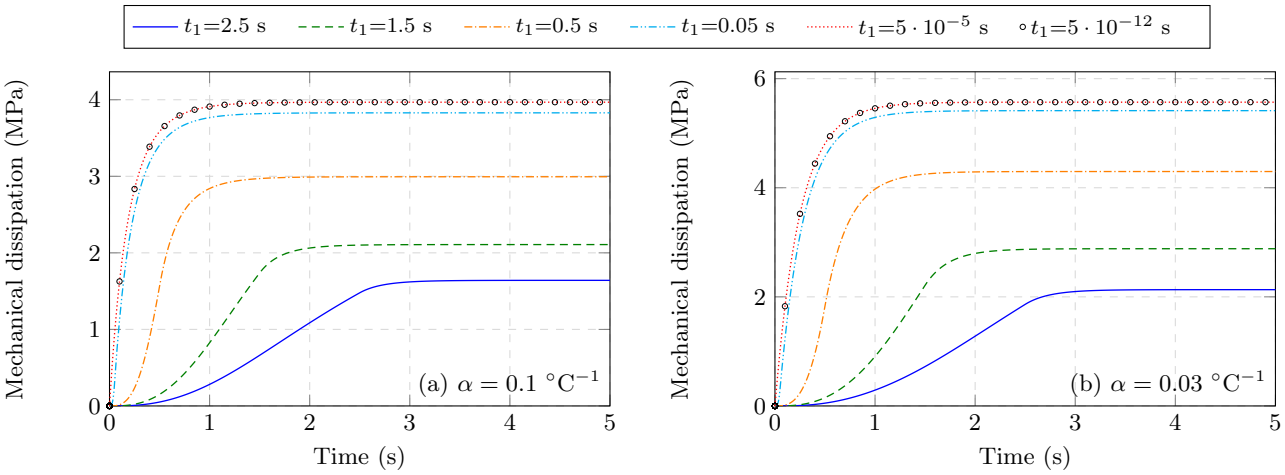

Figure 3. Mechanical dissipations over time for the simple uniaxial creep test

6. ACKNOWLEDGEMENTS

This study was financed in part by the *Coordenação de Aperfeiçoamento de Pessoal de Nível Superior – Brasil* (CAPES) – Finance Code 001 –, the Brazilian agency National Council for Scientific and Technological Development (CNPq) – grant 310482/2016-0 –, and the São Paulo Research Foundation (FAPESP) – Process Number 2018/23957-2. The authors would like to thank them for the financial support given to this research.

7. REFERENCES

Bonet, J., 2001. "Large strain viscoelastic constitutive models". *International Journal of Solids and Structures*, Vol. 38, No. 17, pp. 2953–2968. ISSN 0020-7683. doi:https://doi.org/10.1016/S0020-7683(00)00215-8.

Carvalho, P.R., Coda, H.B. and Sanches, R.A., 2023. "A large strain thermodynamically-based viscoelastic–viscoplastic model with application to finite element analysis of polytetrafluoroethylene (PTFE)". *European Journal of Mechanics - A/Solids*, Vol. 97, p. 104850. ISSN 0997-7538. doi:https://doi.org/10.1016/j.euromechsol.2022.104850.

de Souza Neto, E., Peric, D. and Owen, D., 2011. *Computational Methods for Plasticity: Theory and Applications*. Wiley. ISBN 9781119964544.

Huber, N. and Tsakmakis, C., 2000. "Finite deformation viscoelasticity laws". *Mechanics of Materials*, Vol. 32, pp. 1–18. doi:10.1016/S0167-6636(99)00045-9.

Kamlah, M. and Haupt, P., 1997. "On the macroscopic description of stored energy and self heating during plastic deformation". *International Journal of Plasticity*, Vol. 13, No. 10, pp. 893 – 911. ISSN 0749-6419. doi: https://doi.org/10.1016/S0749-6419(97)00063-6.

Mason, J., Rosakis, A. and Ravichandran, G., 1994. "On the strain and strain rate dependence of the fraction of plastic work converted to heat: an experimental study using high speed infrared detectors and the kolsky bar". *Mechanics of*

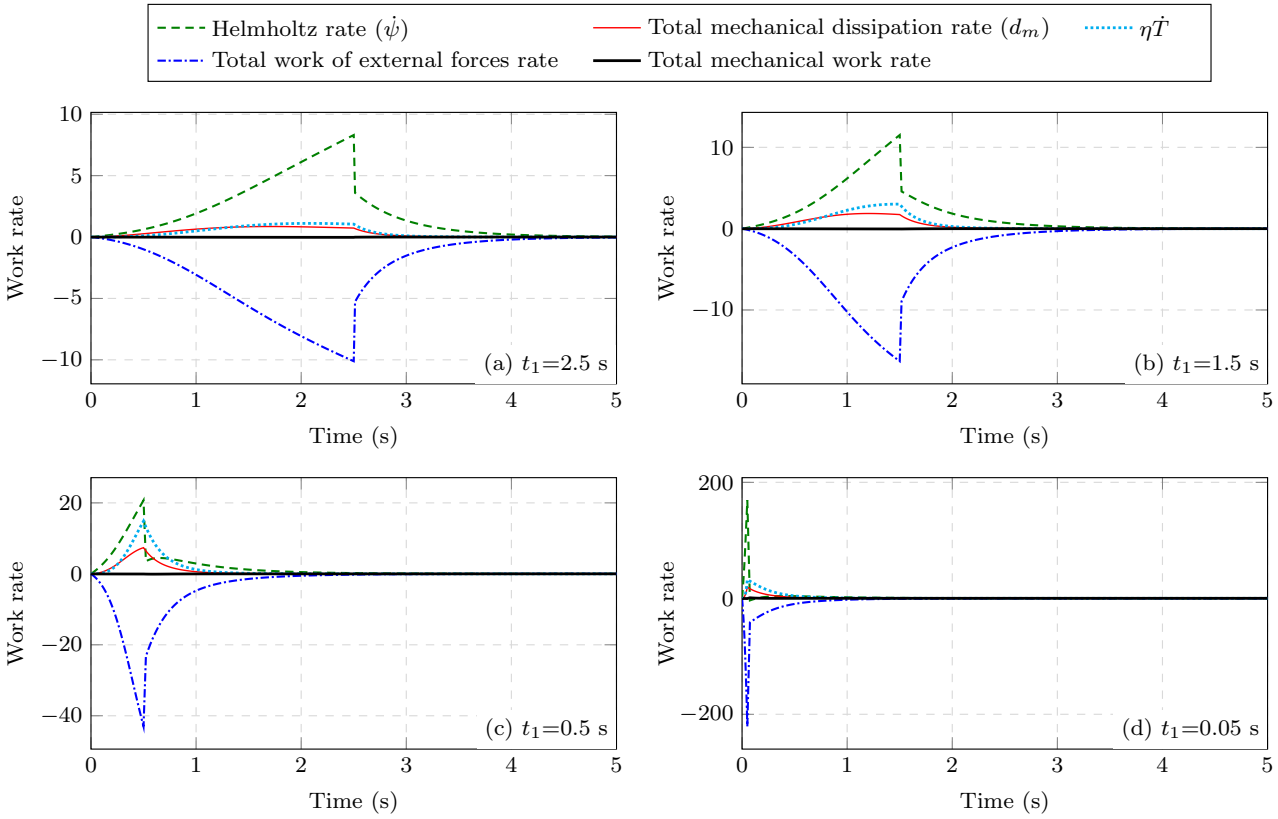

Figure 4. Work rates over time for the simple uniaxial creep test with $\alpha = 0.1°\text{C}^{-1}$

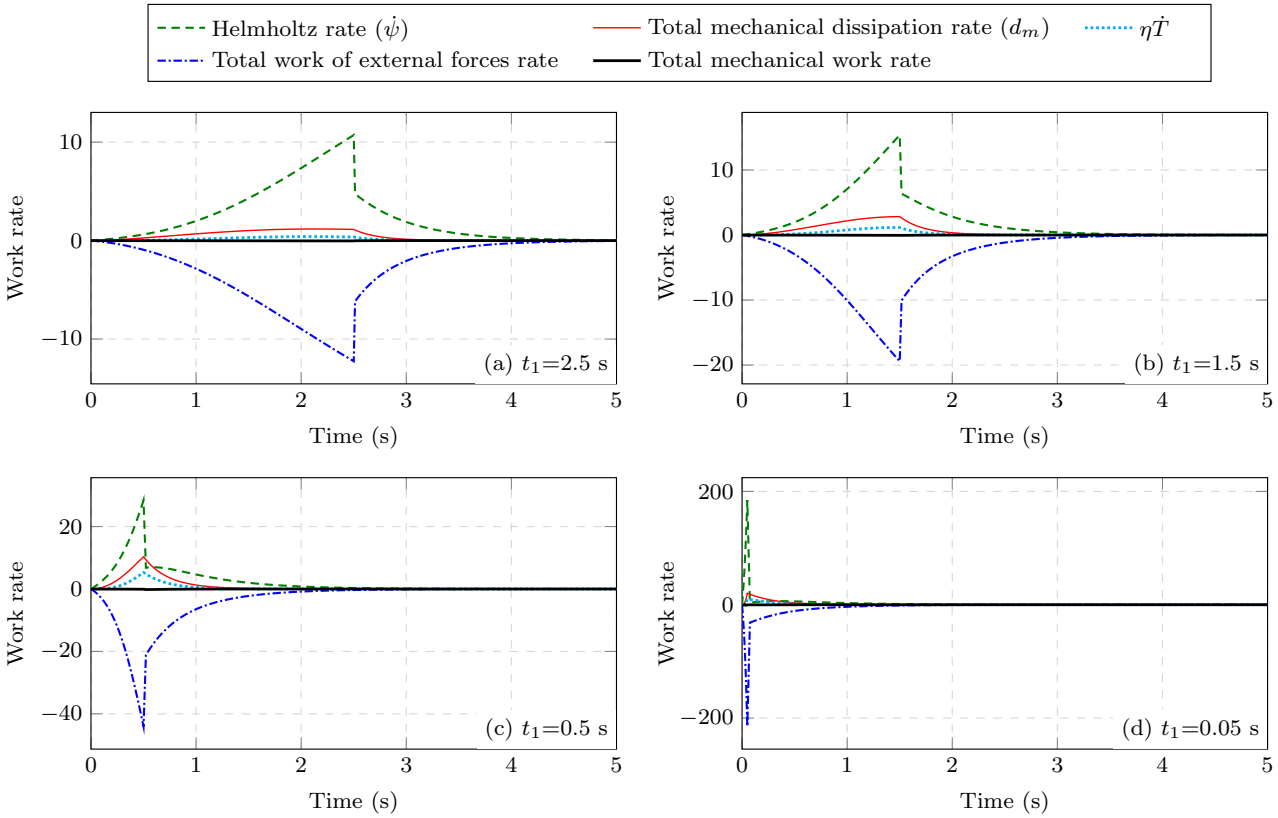

Figure 5. Work rates over time for the simple uniaxial creep test with $\alpha = 0.03°\text{C}^{-1}$

Materials, Vol. 17, No. 2, pp. 135 – 145. ISSN 0167-6636. doi:https://doi.org/10.1016/0167-6636(94)90054-X.

Pascon, J.P. and Coda, H.B., 2017. "Finite deformation analysis of visco-hyperelastic materials via solid tetrahedral finite elements". *Finite Elements in Analysis and Design*, Vol. 133, pp. 25 – 41. ISSN 0168-874X.

Rosakis, P., Rosakis, A., Ravichandran, G. and Hodowany, J., 2000. "A thermodynamic internal variable model for the partition of plastic work into heat and stored energy in metals". *Journal of the Mechanics and Physics of Solids*, Vol. 48, No. 3, pp. 581 – 607. ISSN 0022-5096. doi:https://doi.org/10.1016/S0022-5096(99)00048-4.

Simo, J. and Hughes, T., 2000. *Computational Inelasticity*. Interdisciplinary Applied Mathematics. Springer New York. ISBN 9780387975207.

Vujošević, L. and Lubarda, V., 2002. "Finite-strain thermoelasticity based on multiplicative decomposition of deformation gradient". *Theoretical and applied mechanics*, , No. 28-29, pp. 379–399.

8. RESPONSIBILITY NOTICE

The authors are solely responsible for the printed material included in this paper.